Detection and Classification of Urea Adulteration in Milk with Deep Neural Networks

Ketaki Ghodinde
COEP Technological University, India
ssk.instru@coep.ac.in (corresponding author)

Uttam Chaskar
COEP Technological University, India
umc.instru@coep.ac.in

Received: 17 February 2024 | Revised: 31 March 2024 | Accepted: 7 April 2024

 DOI: https://doi.org/10.48084/etasr.7091

ABSTRACT

Milk is a major food constituent. However, the existing discrepancy between milk demand and supply leads to adulteration, which can be dangerous since it causes detrimental effects on health implicating lethal diseases. Although classical methods for adulteration detection are very accurate, their implementation requires skilled technicians as well as expensive and sophisticated instruments. These reasons trigger the need for improved techniques in uncovering adulteration. Urea is a natural component in milk and accounts for a substantial share of adulteration in the non-protein content of milk. The current research proposes and employs a sensor system utilizing the Electrical Impedance Spectroscopy (EIS) method to determine the presence of urea. The classification system was developed using different machine learning algorithms. Three classifiers, Extreme Gradient Boosting (XGBoost), Extreme Learning Machines (ELM), and Deep Neural Networks (DNN) were considered for various levels of urea adulteration. Milk samples were assessed by deploying the developed EIS sensor assembly and the results derived were employed in the training of the machine learning algorithms. The estimated classifiers displayed promising outcomes, involving up to 98.33% classification accuracies, outshining frequently used existing learning approaches like logistic regression.

Keywords-sensor system development; EIS sensor; milk adulteration; urea detection; deep neural networks; classification

I. INTRODUCTION

Milk is an essential element in the in dietary intake for both children and adults. It is the principal source of calcium and protein in individuals' food. Globally, around 68% of the people consume milk on a regular or semi-regular basis. Milk adulteration has become a serious socio-economic challenge and a universal concern. It has a significant impact on public health causing gastrointestinal disorders, nausea, diarrhoea, allergies, and, in severe cases, even death [1-3]. Some of the commonly used chemical adulterants are high protein compounds, such as whey powder, bone meal, dried egg white, soy protein, and nitrogen-based chemicals, entailing urea, ammonium sulphate, melamine, and dicyandiamide [4]. Adulterants, like detergents, sodium-bi-carbonate, sodium hydroxide, and salts are mostly reported in the developing countries [5]. Preservatives added in the milk are potassium dichromate, hydrogen peroxide, salicylic acid, and benzoic acid. Vegetable oil is mixed with the milk to replace the fat content whereas starch is added to increase solid-non-fat (SNF) [6]. Chemicals like borax, boric acid, hydrated lime, formalin, sugar, and tertiary nitrogen compounds are adulterated in milk [7].

Urea is a natural milk constituent that signifies most of the non-proteinaceous nitrogen. The permitted level for urea is about 70 mg in 100 ml of milk [8]. Near infrared Raman spectroscopy, Liquid chromatography, Gas Chromatography/Isotope Dilution Mass Spectrometry (GC/IDMS), High Pressure Liquid Chromatography (HPLC) techniques can quantify the naturally occurring and deliberately added urea [9-12]. Kjeldhal and Dumas method, UV-visible spectrophotometry, Fourier Transform Infrared Spectroscopy (FTIR), and Surface-Enhanced Raman spectroscopy (SERS) are useful for protein analysis in the raw milk [13, 14]. These analytical techniques are highly sophisticated and have high sensitivity. Nevertheless, these tests are confined to laboratories, are time consuming, and are not suitable for large-scale analysis [14]. Many of these tests cannot differentiate between milk protein and extraneous added nitrogen contents [13]. As an alternative approach, the fatty acid profile of milk

is used in Gas Chromatography through Flame Ionization Detection (GC-FID). Capillary zone Electrophoresis (CE) with ultraviolet (UV) identification has also been employed for classification [15]. VIS (visible) and NIR (Near Infrared) spectroscopy can quantify the milk quality [16]. To deal with some of the limitations of these analytical methods, novel sensing methods are proposed. A capacitive sensor, sensitive to electrical properties, gives different dielectric loss angle values measured by immersing the sensor in the milk [17]. Electrical Impedance Spectroscopy (EIS) deals with the electrical impedance of milk and characterizes the ultra-pasteurized milk [18]. The EIS technique is unmalicious, its multi-dimensional data can be analyzed with statistical or chemometric methods for screening of adulteration in milk [19]. Electrochemical biosensing is employed for urea detection in milk with three electrochemical methods like Cyclic Voltammetry (CV), chronoamperometry (CA), and Differential Pulse Voltammetry (DPV) [20]. These techniques deliver a rapid response and achieve a good Level of Detection (LoD) according to the Food Safety and Standard Authority of India (FSSAI) [21]. In recent years, many chemometric methods have been devised for supervised pattern recognition. Support Vector Machines (SVMs) and Artificial Neural Networks (ANNs) aid in the NIR spectroscopy analysis. In contrast to traditional analysis, NIR spectroscopy is combined by One Class Partial Least Squares (OCPLS) classifier employed in the rapid screening of the melamine in milk [22]. Chemometric tools with investigative analysis and pattern recognition, such as Principal Component Analysis (PCA), interpret the data of Partial Least Square Discriminant Analysis (PLSDA). All the mentioned techniques are applied in the classification of milk / milk powder adulteration [23]. Standardized analysis of milk adulteration is an expensive and laborious process. Recent techniques, such as electronic nose in conjunction with chemometrics are proven to be efficient tools regarding the classification of milk [24]. Machine Learning (ML) methods like ANNs have better performance than classical prediction methods in the dairy sector. Differential scanning calorimeter is used to predict the nutritional and physicochemical properties with the help of ML techniques, like Gradient boosting machine, Random Forest (RF), and Multilayer Perceptron (MLP) [25]. These techniques are beneficial in the detection of adulterants, such as starch, whey, formaldehyde, and urea in the milk [26]. Hyper spectral sensing and ML for identification of spectral signatures are applied for milk quality detection [27]. A synthesis of pH sensitive nanofibers incorporated in nylon-6 solution was electrically spun in the milk adulteration and the sensors were optimized with SVMs for classification of images captured by a smartphone camera [28]. FTIR spectral data for sample milk were explored with ML approaches like ANNs and Decision Trees (DTs) to characterise the features of contaminated milk [29]. EIS data were assessed by Multi-Dimensional Scaling (MDS) clustering and visualization algorithms in [30-32]. The training data provided to the model are a crucial factor that determines how the ML model performs. There are no publicly available datasets for milk adulterants. Collecting and curating large milk adulterant datasets for the ML algorithm development is typically difficult and resource intensive. The current paper elaborates the sensing assembly with the EIS technique for the generation of training and testing data. Three ML algorithms were compared regarding classification accuracy. This developed method is rapid and cost effective.

II. MATERIALS AND METHODS

A. Electrochemical Impedance Spectroscopy (EIS) Sensor Assembly

Electrochemical cells with different numbers of electrodes of various materials can be used to analyze the electrochemical behavior of the electrode material and the electrolyte. In the simplest format, two electrodes of the same/different material are applied with a small alternating electrical signal and are dipped in electrolyte solution, which, in this case, is pure and urea adulterated cow milk. The output electrical response of the cell depends on the conducting properties of the electrodes, namely electron kinetics, transfer rate of electrons from the electrodes to the electrolyte, and the rate of redox reaction. The interaction resistance of the electrodes and electrolyte decides the rate of flow of ions and electrons. The impedance values are observed by applying AC voltage at different frequencies. The electrical impedance, which is a pseudo-linear response of the electrochemical cell, acts as an obstacle to the passage of the AC current. This response can be represented as:

$$Z = \frac{E_t}{I_t} = \frac{E_0 \sin(\omega t)}{I_0 \sin(\omega t + \emptyset)} = Z_0 \frac{\sin(\omega t)}{\sin(\omega t + \emptyset)} \quad (1)$$

where Z_0 is the magnitude and $\emptyset$ is the phase shift of the impedance signal, E_t and I_t are the AC potential and current at time t, E_0 and I_0 represent the maximum signal amplitude, and ω denotes the radial frequency. The complex form of the same response can be written as:

$$Z(\omega) = Z_0 \, exp(j\emptyset) = Z_0(cos\,\emptyset + j\,sin\,\emptyset) \quad (2)$$

There are two standard methods to plot the cell response. In a Nyquist plot, the real and imaginary parts of the response are ubiquitous. In the Bode plot, the impedance amplitude and phase shift are plotted against frequency on a logarithmic scale. Figure 1 displays the EIS sensor which forms the electrochemical cells. It consists of two parallel rods of SS-316, which are dipped in electrolyte, which is milk.

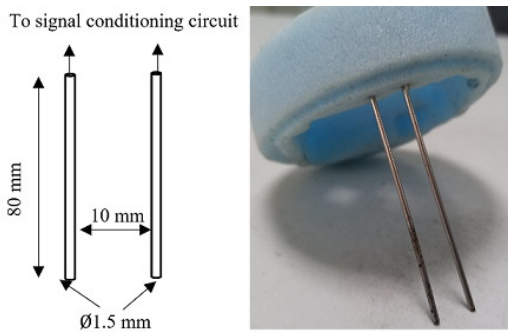

Fig. 1. EIS sensor details.

AC voltage is applied to the sensor electrodes and the output parameter (either impedance or voltage proportional to impedance) is monitored. If complexities like the deposition on the electrodes, and the kinetics of redox reaction are ignored, the electrical equivalent of the sensor is a series-parallel

combination of capacitors and resistances. For the measurement of EIS sensor response two different methods are followed:

- Impedance measurement with an LCR meter.
- Phase measurement with a designed electronic assembly.

B. Impedance Measurement with the LCR Meter

The EIS sensor employed in the experiment has the dimensions mentioned in Figure 1. During measurement, two electrodes of the sensor are kept 10 mm apart and are immersed in milk by 20 mm [30]. As this is a food application, the sensor is not coated with any activating enzymes. The sensor impedance in the electrolyte is calculated with the help of Aplab to make 4910 LCR meter. Noting the resistance and capacitance using (3), impedance for different values of frequency can be calculated. This experimentation aids in plotting the EIS spectrum for resistance, capacitance, and impedance values for a varying frequency.

C. Phase Measurement with Sensor Assembly

Figure 2 manifests the experimental setup to solve the portability problem and avoid the use of costly instruments like LCR meters. Changes of the phase angle (i.e. changes in impedance) are converted into voltage signal with the proposed electronic circuit [5]. The phase angle and, so, the voltage produced, change due to alterations in the urea adulteration in milk. The phase shift measurement is the comparison of the input AC signal and the output AC signal phase angle. The 1VAC is applied to the sensor from the function generator, Insek make model no. AFG 2225. The sensor output signal is connected to the limited gain amplifier circuit and then to the open loop gain amplifier. Similarly, the input AC signal of 1Vpp is also connected in similar fashion. These two signals, which are square waves, are then fed to the XOR gate to generate voltage corresponding to phase shift after the R-C filter. The generated voltage is caused by a phase difference between the output and the input signals caused by changes in the composition of milk. Figure 3 exhibits a graph of different voltage values for various levels of urea adulteration.

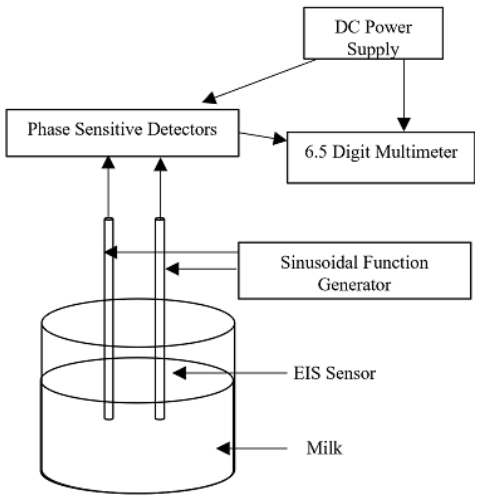

Fig. 2. Block diagram of phase angle measurement procedure.

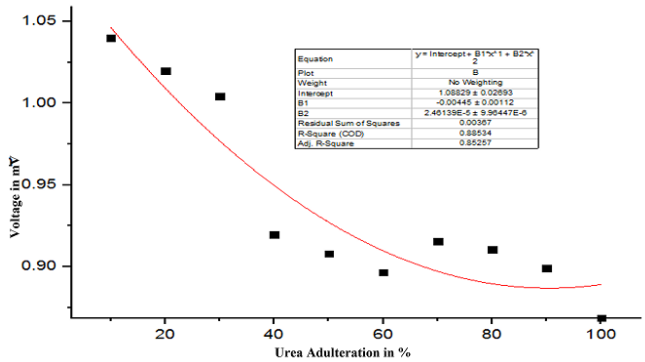

Fig. 3. Phase angle measurement: urea detection results.

D. Adulteration Classification Methodology

The experimental results reveal a typical pattern of the output values. This fact encouraged this study to develop an ML classification system. The algorithms selected are XGBoost, ELM (Extreme Learning Machines), and DNNs (Deep Neural Networks). These algorithms are applied for some food quality classification, but not for milk. These algorithms are employed for the classification of EIS data for the first time.

1) XGBoost Classification Model

XGBoost is a robust approach commonly used for classification and regression models. It mainly depends upon the gradient boosting structure [33]. This continuously adds novel DTs for fitting values with the remaining multiple iterations, enhancing the performance and efficiency of the learner. XGBoost is different from gradient boosting as it employs a Taylor extension for approximating the loss function. The algorithm contains a good trade-off between variance and bias, generally utilizing less DTs to attain a high precision [34]. Consider a sample set consisting of m features and n samples. It is formulated by $D = \{(x_i, y_i)\}(|D| = n, x_i \in R^m, y_i \in R)$, whereas y denotes the true value and x represents the eigen value. The model sums the result of K trees as the last prediction values, as follows.

$$\hat{y}_i = \sum_{k=1}^{K} \quad f_k(x_i), f_k \in F \tag{3}$$

where F represents the collection of DT models

$$F = \{f(x) = w_{q(x)}\}(q: R^m \to T, w \in R^T) \tag{4}$$

where $w_{q(x)}$ represents the weight of the leaf node and $f(x)$ indicates a tree. T specifies the quantity of leaf nodes and q is the framework of all trees that map the samples to the respective leaf nodes. Thus, the prediction values of XGBoost are the amount of the values of the leaf node of all the trees [30]. The aim of the algorithm is to learn these k trees, by minimizing the succeeding objective function:

$$L^{(t)} = \sum_{i=1}^{n} l(y_i, \hat{y}_i) + \sum_{k=1}^{K} \Omega(f_k) \tag{5}$$

where l represents the variation loss among the true value y_i and the estimated values $\hat{y}_i$, the general loss function includes the square, exponential, and logarithmic loss functions. Ω

normalization is utilized for setting the penalty of the DTs to avoid overfitting. Ω is formulated by:

$$\Omega(f) = \gamma T + \frac{1}{2}\lambda\|\omega\|^2 \quad (6)$$

In the constant term, γ represents the hyperparameters which control the complication of the algorithm and T represents the leaf node amount. λ indicates the penalty coefficients of leaf weight ω, which is generally constant. λ and ω determine the complication of the algorithm and are generally provided empirically. At the time of training, novel trees are included for fitting the residual of the earlier rounds. Thus, once the algorithm contains t trees, it can be written in the form:

$$\hat{y}_i^{(t)} = \hat{y}_i^{(t-1)} + f_k(x_i) \quad (7)$$

Substituting (4) to the objective function (2), we get:

$$L^{(t)} = \sum_{i=1}^{n} l\left(y_i, \hat{y}_i^{(t-1)} + f_t(x_i)\right) + \Omega(f_k) \quad (8)$$

XGBoost performs the Taylor extension of the objective function comprising three terms:

$$L^{(t)} \approx$$

$$\sum_{i=1}^{n}\left[l\left(y_i, \hat{y}^{(t-1)}\right) + g_i f_t(x_i) + \frac{1}{2}h_i f_t^2(x_i)\right] + \Omega \quad (9)$$

where g_i represents the initial derivatives and h_i denotes the second derivative of the loss function. The residuals among the predictive scores $\hat{y}^{(t-1)}$ and y_i do not influence the objective function optimization, hence they are eliminated:

$$\tilde{L}^{(t)} = \sum_{i=1}^{n}[g_i f_i(x_i) + \frac{1}{2}h_i f_i^2(x_i)] + \Omega(f_k) \quad (10)$$

The iterations of the tree algorithm are converted to the iterations of the leaf node, and the estimated optimum leaf node scores are: $G_j^2/(H_j + \lambda)$. By replacing the optimum value with the objective function, the following last objective function is attained:

$$Obj = \frac{1}{2}\sum_{j=1}^{T}\frac{G_j^2}{H_j+\lambda} + \gamma T \quad (11)$$

Generally, XGBoost adds standardization to the normal function due to its low computational complexity.

2) ELM Classification Model

This subsection briefly discusses the typical ELM based classification model [35, 36]. ELM was initially developed for the SLFN model. For N random distinctive samples (x_i, t_i), let $x_i = [x_{i1}, x_{i2}, \dots, x_{id}]^T \in R^d$ and $t_i = [t_{i1}, t_{i2}, \dots, t_{im}]^T \in R^m$, the typical SLFNs using $\widetilde{N}$ hidden nodes and activation function $g(x)$ are arithmetically modelled as follows:

$$\sum_{i=1}^{\widetilde{N}}\beta_i g(x_j) = \sum_{i=1}^{\widetilde{N}}\beta_i g(w_i \cdot x_j + b_i) = o_j \quad (12)$$

where $j = 1, \dots, N$, $w_i = [w_{i1}, w_{i2}, \dots, w_{iN}]^T$ represents weight vectors linking the i^{th} hidden and input nodes, $\beta_i = [\beta_{i1}, \beta_{i2}, \dots, \beta_{im}]^T$ denotes the weight vectors linking the i^{th} hidden and the output nodes, and b_i signifies the thresholding of the i^{th} hidden node. The SLFN using N hidden nodes with $g(x)$ activation function was able to estimate the N instances with zero error [35], implying that $\sum_{j=1}^{\widetilde{N}}\|o_j - t_j\| = 0$, i.e., there are β_i, w_i, b_i such that:

$$\sum_{i=1}^{\widetilde{N}}\beta_i g(w_i \cdot x_j + b_i) = t_j\ , j = 1, \dots, N \quad (13)$$

$$H\beta = T \quad (14)$$

Let:

$$H = [h(x_1) \vdots h(x_N)] = [g(w_1 \cdot x_1 + b_1) \cdots g(w_{\widetilde{N}} \cdot x_1 + b_{\widetilde{N}}) \vdots \ddots \vdots g(w_1 \cdot x_N + b_1) \cdots g(w_{\widetilde{N}} \cdot x_N + b_{\widetilde{N}})]_{N\times\widetilde{N}} \quad (15)$$

$$\beta = \left[\beta_1^T \vdots \beta_{\widetilde{N}}^T\right]_{\widetilde{N}\times m} and\ T = [t_1^T \vdots t_N^T]_{N\times m} \quad (16)$$

where H is the SLFN hidden layer output matrix and the i^{th} column of H represents the i^{th} output of the hidden node regarding the input $x_1, x_2, \dots, x_N$. It is shown in [35] that once the activation function g is substantially distinguishable in some intervals, the hidden layer parameter is arbitrarily produced. Hence, (11) turns into a linear method and the β output weight is evaluated by:

$$\hat{\beta} = H^{\dagger}\mathrm{T} \quad (18)$$

Therefore, the ELM first arbitrarily produces the parameter hidden node and then systematically computes the output weight β and the hidden layer output matrix [37]. The former prevents some longer training process wherever the SLFN hidden layer needs to be adjusted. In comparison with the conventional ML models, the ELM achieves good generalization efficiency at a fast-learning speed with less human involvement.

3) The DNN Classification Model

An AE is a feedforward ANN which includes one output, one input, and one hidden layer. In the AE, the input and output dimensions are equal. The training of the AE takes place by embedding the input space to the code (feature) space where the dimensions are usually lesser. The AE tries to give a good demonstration of the input vectors by substituting them with a suitable code [38]. The M-dimension input vector is determined by $x^{(1)}, x^{(2)} \dots x^{(\mathrm{T})}$ whereas the number of neurons in the hidden layer is N. T denotes the amount of input vectors. AE's left side is known as the encoder, where the hidden layer is the output of the AE and the input is the input of the AE. The encoder converts a provided input vector to a code, aiming to an effective depiction of the input vector [38]. The relationship between the output and the input of the encoder is equated as $c = g_E(W, b; x)$. Furthermore, it can be determined by:

$$c = f(b + W^T x) \quad (19)$$

where f represents the activation function of the encoder neuron. The AE's right side is the decoder, where the output $\hat{x}$ represents the output of the AE and the input is the output of the hidden layer (c). The decoder using the $\widehat{W}$ weight matrix and the vector $\hat{b}$ converts the provided code vectors to the inventive input vectors. The encoder's output and input relationships can be given by:

$$\hat{x} = \hat{f}\left(\hat{b} + \widehat{W}^T c\right) \quad (20)$$

where $\hat{f}$ represents the activated R function of the decoder neuron. The relationship between the output and the input of the decoder can be represented as $\hat{x} = g_D(\widehat{W}, \hat{b}; c)$. The output of the AE is formulated as $\hat{x} = g_{AE}(W, b, \widehat{W}, \hat{b}; x)$. The objective function of the AE can be determined by:

$$E_{sparse} = E_T + \beta \sum_{j=1}^{N} KL(\rho \| \hat{\rho}_j) \quad (21)$$

The above-mentioned cost function consists of two parts. The initial part E_T is determined below and is an objective function of an ANN [36], whereas β represents the sparsity penalty weight seen in (18):

$$E_T = \frac{1}{T}\sum_{k=1}^{T} e_k^2 + \frac{\lambda}{2}\left(\|W\| + \|\widehat{W}\|\right) \quad (22)$$

Let us consider λ to be a standardization term utilized for preventing overfitting. The error vectors are the variation among the desirable and the original output:

$$e_k = \|x^{(k)} - \hat{x}^{(k)}\| \quad (23)$$

whereas $k = 1,2, \ldots T$. It is easier to observe that E_T denotes an internal weight function of the AE like $E_T = E_{AE}(W, b, \widehat{W}, \hat{b})$. The next portion of (18), called Kullback-Leibler divergence $KL(\rho \| \hat{\rho}_j)$, can be provided by:

$$KL(\rho \| \hat{\rho}_j) = \rho log \frac{\rho}{\hat{\rho}_j} + (1-\rho) log \frac{1-\rho}{1-\hat{\rho}_j} \quad (24)$$

$$\hat{\rho}_j = \frac{1}{T}\sum_{i=1}^{T} f_j\left(x^{(i)}\right) \quad (25)$$

The common training process of DNN can be implemented with a dataset where $\{x^{(1)}, x^{(2)}, \ldots, x^{(T)}\}$ denote the input vector and $\{y^{(1)}, y^{(2)}, \ldots, y^{(T)}\}$ denote the target value demonstrating the class label related to the respective input vector.

III. EXPERIMENTAL VALIDATION

The proposed model's performance is validated with the milk data and the results are investigated in terms of different measures, namely accuracy (ACC_Y), precision (PRE_N), recall (REC_L), F-measure $(F_{measure})$, kappa, Area Under the Curve (AUC), and ROC. In addition to this, a brief comparative analysis of the three proposed models with the existing ones takes place to highlight the improved performance of the proposed model. The simulation setup, dataset details and results are elaborated in the following sections.

IV. IMPLEMENTATION DETAILS

The proposed model is implemented on a PC i5-8600k, MSI Z370 A-Pro, GeForce 1050 Ti 4GB, 16 GB RAM, and 1 TB HDD. This model is simulated in Python 3.6.5 with tensorflow-gpu 2.2.0, pandas, pyqt5, prettytable, tqdm, xgboost, scikit-elm, matplotlib, seaborn, scikit-learn, dask, dask[distributed], openpyxl, and numpy 1.19.5 packages. In addition, the recommended model was tested using a dataset that includes numerous instances under 6 class labels, namely No urea (Class 0), 4 mg urea (Class 1), 8 mg urea (Class 2), 12 mg urea (Class 3), 16 mg urea (Class 4), and 20 mg urea (Class 5). The dataset contains a set of 10 samples under each class. The attributes involved in the dataset are frequency, voltage, resistance, capacitance, reactance, and impedance.

V. RESULTS

A. Result Analysis of the XGBoost Model

The confusion matrix of the XGBoost technique is shown in Figure 4. The XGBoost model has classified 9 samples into Class 0, 10 samples into Class 1, 10 samples into Class 2, 10 samples into Class 3, 9 samples into Class 4, and 10 instances into Class 5. The ROC analysis of the XGBoost model on milk data classification is portrayed in Figure 5. The results show that the XGBoost model has obtained a high ROC of 0.99, 1.00, 1.00, 1.00, 1.00, and 1.00 on sample classification. From these values, it is ensured that the XGBoost model has properly classified the dataset.

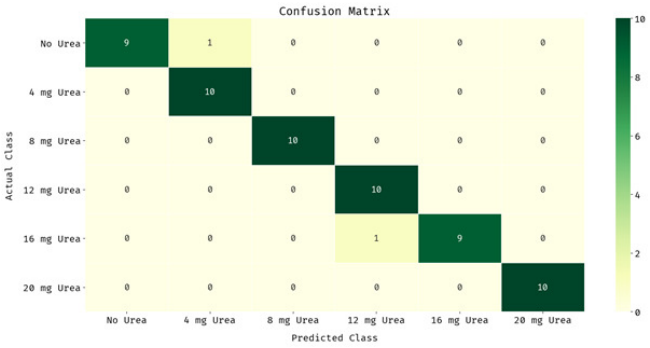

Fig. 4. Confusion matrix of the XGBoost model.

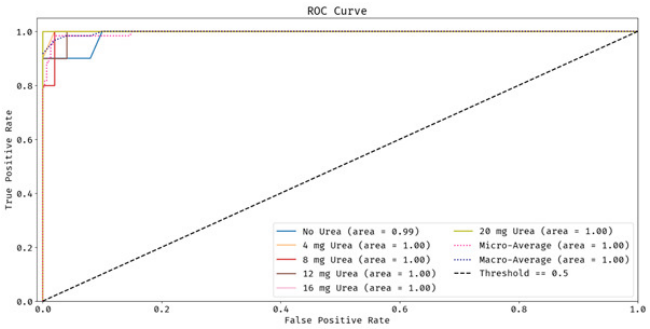

Fig. 5. ROC analysis of the XGBoost model on milk classification.

B. Result Analysis of the ELM Model

Figure 6 presents the confusion matrix produced by the ELM model.

Fig. 6. Confusion matrix of the ELM model.

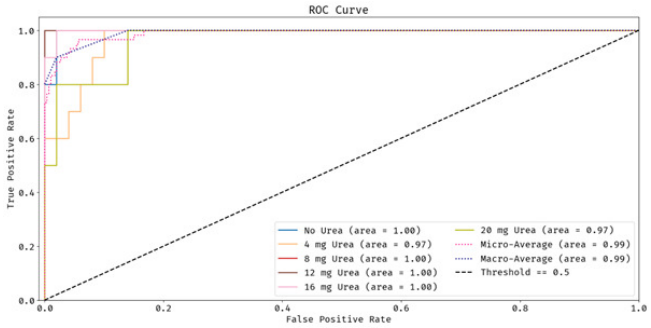

Fig. 7. ROC analysis of the ELM model on milk classification.

It demonstrates that the ELM model has classified 10 samples into Class 0, 9 samples into Class 1, 10 samples into Class 2, 10 samples into Class 3, 10 samples into Class 4, and 8 samples into Class 5. The ELM model's ROC analysis is presented in Figure 7 with values that are found to be considerably high.

C. Result Analysis of the DNN Model

The confusion matrix generated by the DNN model is depicted in Figure 8. The DNN model has proficiently categorized 10 samples into Class 0, 9 samples into Class 1, 10 samples into Class 2, 10 samples into Class 3, 10 samples into Class 4, and 10 samples into Class 5. The ROC analysis of the DNN model is showcased in Figure 11. The results indicate that the DNN model has led to an increased ROC of 1.00, 1.00, 1.00, 1.00, 1.00, and 1.00 on the classification of the samples. These ROC values ensure that the DNN model has accomplished higher ROC values than the XGBoost and ELM models. Figure 9 displays the accuracy graph of the DNN approach on the test milk classification data. It shows that DNN model's training and validation accuracy increase when the epoch count increases. It should be also noted that the validation accuracy is found to be slightly higher than the training accuracy.

The loss graph analysis of the DNN technique on the test milk dataset is portrayed in Figure 10. It points out that the DNN model has led to reduced training and validation loss, with the former being considerably lower than the latter.

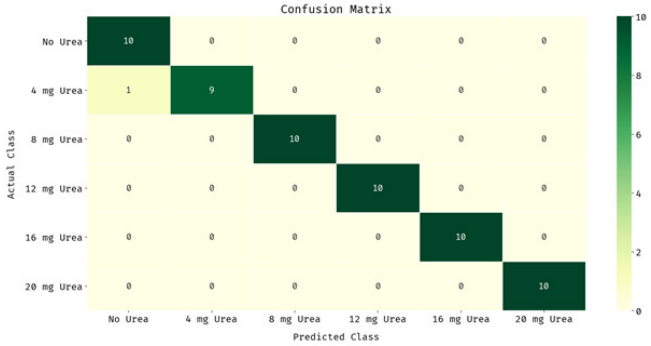

Fig. 8. Confusion matrix of the DNN model.

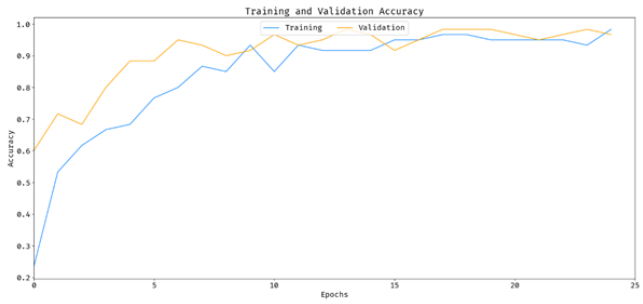

Fig. 9. Accuracy graph analysis of the DNN model

Fig. 10. Loss graph analysis of the DNN model.

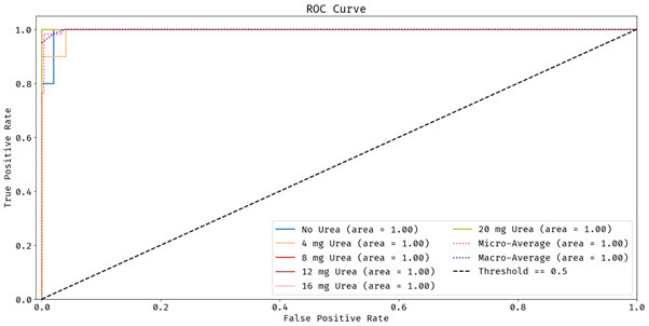

Fig. 11. ROC analysis of the DNN model on milk classification.

VI. DISCUSSION

A comparative study of the accuracy percentage of the developed models with some earlier used models (specialized in food applications) is provided in Table I. The accuracy analysis of the different models manifests that the RF and Logistic Regression (LR) models obtained lower performance over the other techniques with ACC_Y of 81% and 72.80%. Besides this, the Adaboost technique has accomplished a slightly enhanced ACC_Y of 92.60%. Moreover, the ELM and XGBoost techniques attained a moderately higher ACC_Y of 95% and 96.67% respectively. However, the DNN model has demonstrated the best outcome with the highest ACC_Y of 98.33%.

The classification result analysis of the considered three classification models in terms of different metrics is offered in Table II. The results exhibited that the ELM model had showcased ineffective outcomes over the other techniques with minimal classification results. At the same time, the XGBoost model had displayed reasonably closer classification results

over the ELM model. However, the DNN model had surpassed the other two classifiers.

TABLE I. ACCURACY COMPARISON WITH EARIER USED MODELS OF THE PROPOSED MILK CLASSIFICATION

Model	Accuracy (%)
DNN	98.33
ELM	95.00
XGBoost	96.67
RF	72.80
LR	81.00
Adaboost	92.60

TABLE II. CLASSIFICATION RESULT ANALYSIS OF THE CONSIDERED MODELS

Methods	DNN (%)	ELM (%)	XGBoost (%)
ACC_Y	98.33	95.00	96.67
PRE_N	98.48	96.15	96.97
REC_L	98.33	95.00	96.97
$F_{measure}$	98.33	95.10	96.66
KAPPA	98.00	94.00	96.00
AUC	99.87	98.87	99.70

From the values in Table II, it is evident that the DNN model has attained an enhanced outcome as compared to the ELM and XGBoost models. After studying the aforementioned results, it can be concluded that the DNN model has the ability to outperform the other methods on milk data classification due to its automated feature engineering process. Thus, the DNN model could be utilized as a proficient technique in determining milk quality in real world applications.

VII. CONCLUSION

The current paper presented a novel hardware and software approach in the detection of urea adulteration in cow milk. It uses Electrochemical Impedance Spectroscopy (EIS) and machine learning techniques for classification. The sensor setup contains an EIS sensor and a signal conditioning circuit, which converts the impedance of the sensor into voltage. The impedance variations that differ in the phase angle of the output signal of the sensor, aid in the identification of milk mixed with varying urea percentages. The frequency obtained in the detection process was confirmed and the transformation of the degree of adulteration onto resistance, impedance, and phase angle were examined by using the derived technique. In previous works, urea quantification in water was carried out by modeling the EIS sensor for its electrical circuit in the LEVMW software. Another research where similar sensors were deployed for detection of fat percentage [5] classified the milk with the help of the EIS analyzer software. The EIS sensor assembly with the signal conditioning circuit is a novel contribution on the hardware side.

The utilized classification models (XGBoost, ELM, and DNN) have not been previously used in dairy or food applications. This paper compares these models with other known models like Adaboost and Random Forest, which have been utilized in earlier works and food applications. The implemented XGBoost, ELM, and DNN exhibited better accuracy values than the other models. Among the deployed models, DNN exhibited the best accuracy of 99%. Thus, a simple sensor system along with these classification models permits urea detection up to 70 mg per 100 ml of milk, accomplishing a Level of Detection (LOD) in accordance with the FSSAI standards. Finally, the portable system design has a simple electronic circuitry and promotes low cost.

REFERENCES

[1] A. F. S. Silva and F. R. P. Rocha, "A novel approach to detect milk adulteration based on the determination of protein content by smartphone-based digital image colorimetry," *Food Control*, vol. 115, Sep. 2020, Art. no. 107299, https://doi.org/10.1016/j.foodcont.2020.107299.

[2] T. Azad and S. Ahmed, "Common milk adulteration and their detection techniques," *International Journal of Food Contamination*, vol. 3, no. 1, Dec. 2016, Art. no. 22, https://doi.org/10.1186/s40550-016-0045-3.

[3] Y. Yang *et al.*, "Fraud vulnerability in the Dutch milk supply chain: Assessments of farmers, processors and retailers," *Food Control*, vol. 95, pp. 308–317, Jan. 2019, https://doi.org/10.1016/j.foodcont.2018.08.019.

[4] J. Qin *et al.*, "Detection and quantification of adulterants in milk powder using a high-throughput Raman chemical imaging technique," *Food Additives & Contaminants: Part A*, vol. 34, no. 2, pp. 152–161, Feb. 2017, https://doi.org/10.1080/19440049.2016.1263880.

[5] M. Chakraborty and K. Biswas, "Limit of Detection for Five Common Adulterants in Milk: A Study With Different Fat Percent," *IEEE Sensors Journal*, vol. 18, no. 6, pp. 2395–2403, Mar. 2018, https://doi.org/10.1109/JSEN.2018.2794764.

[6] R. Nagraik, A. Sharma, D. Kumar, P. Chawla, and A. P. Kumar, "Milk adulterant detection: Conventional and biosensor based approaches: A review," *Sensing and Bio-Sensing Research*, vol. 33, Aug. 2021, Art. no. 100433, https://doi.org/10.1016/j.sbsr.2021.100433.

[7] S. Tripathy, A. R. Ghole, K. Deep, S. R. K. Vanjari, and S. G. Singh, "A comprehensive approach for milk adulteration detection using inherent bio-physical properties as 'Universal Markers': Towards a miniaturized adulteration detection platform," *Food Chemistry*, vol. 217, pp. 756–765, Feb. 2017, https://doi.org/10.1016/j.foodchem.2016.09.037.

[8] R. Sharma, Y. S. Rajput, and A. K. Barui, *Detection of Adulterants in milk: A Laboratory Manual (Revised edition)*, NDRI, 2012.

[9] K. M. Khan, H. Krishna, S. K. Majumder, and P. K. Gupta, "Detection of Urea Adulteration in Milk Using Near-Infrared Raman Spectroscopy," *Food Analytical Methods*, vol. 8, no. 1, pp. 93–102, Jan. 2015, https://doi.org/10.1007/s12161-014-9873-z.

[10] X. Dai *et al.*, "Determination of Urea in Milk by Liquid Chromatography-Isotope Dilution Mass Spectrometry," *Analytical Letters*, vol. 45, no. 12, pp. 1557–1565, Aug. 2012, https://doi.org/10.1080/00032719.2012.677779.

[11] X. Dai *et al.*, "Accurate analysis of urea in milk and milk powder by isotope dilution gas chromatography–mass spectrometry," *Journal of Chromatography B*, vol. 878, no. 19, pp. 1634–1638, Jun. 2010, https://doi.org/10.1016/j.jchromb.2010.04.005.

[12] M. Czauderna and J. Kowalczyk, "Easy and accurate determination of urea in milk, blood plasma, urine and selected diets of mammals by high-performance liquid chromatography with photodiode array detection preceded by pre-column derivatization," *Chemia Analityczna*, vol. 54, no. 5, pp. 919–937, 2009.

[13] S. Sen, Z. Dundar, O. Uncu, and B. Ozen, "Potential of Fourier-transform infrared spectroscopy in adulteration detection and quality assessment in buffalo and goat milks," *Microchemical Journal*, vol. 166, Jul. 2021, Art. no. 106207, https://doi.org/10.1016/j.microc.2021.106207.

[14] S. R. Karunathilaka, B. J. Yakes, K. He, L. Bruckner, and M. M. Mossoba, "First use of handheld Raman spectroscopic devices and on-board chemometric analysis for the detection of milk powder adulteration," *Food Control*, vol. 92, pp. 137–146, Oct. 2018, https://doi.org/10.1016/j.foodcont.2018.04.046.

[15] T. de Oliveira Mendes, B. L. S. Porto, M. J. V. Bell, I. T. Perrone, and M. A. L. de Oliveira, "Capillary zone electrophoresis for fatty acids with chemometrics for the determination of milk adulteration by whey

addition," *Food Chemistry*, vol. 213, pp. 647–653, Dec. 2016, https://doi.org/10.1016/j.foodchem.2016.07.035.

[16] N. Kamil *et al.*, "Investigating the Quality of Milk using Spectrometry Technique and Scattering Theory," *Engineering, Technology & Applied Science Research*, vol. 11, no. 3, pp. 7111–7117, Jun. 2021, https://doi.org/10.48084/etasr.4084.

[17] D. Worku, M. Sharma, P. Kumar, and B. Koteswararao, "Detection of Adulteration in milk using capacitor sensor with especially focusing on Electrical properties of the milk.," in *7th International Electronic Conference on Sensors and Applications*, Nov. 2020, pp. 1–10, https://doi.org/10.3390/ecsa-7-08254.

[18] A. M. Lopes, J. A. T. Machado, E. Ramalho, and V. Silva, "Milk Characterization Using Electrical Impedance Spectroscopy and Fractional Models," *Food Analytical Methods*, vol. 11, no. 3, pp. 901–912, Mar. 2018, https://doi.org/10.1007/s12161-017-1054-4.

[19] H. Bouzidi, L. Otmani, R. Doufnoune, L. Zerroual, and D. Benachour, "Influence of Membrane Type on Some Electrical Properties of a Single Microbial Fuel Cell," *Engineering, Technology & Applied Science Research*, vol. 12, no. 3, pp. 8492–8499, Jun. 2022, https://doi.org/10.48084/etasr.4813.

[20] M. Ghasemi-Varnamkhasti, N. Ghatreh-Samani, M. Naderi-Boldaji, M. Forina, and M. Bonyadian, "Development of two dielectric sensors coupled with computational techniques for detecting milk adulteration," *Computers and Electronics in Agriculture*, vol. 140, pp. 266–278, Aug. 2017, https://doi.org/10.1016/j.compag.2017.06.005.

[21] K. A. Ghodinde and U. M. Chaskar, "Quantification of Urea Adulteration with Impedance Spectroscopy in Cow Milk," in *6th International Conference for Convergence in Technology*, Maharashtra, India, Apr. 2021, pp. 1–5, https://doi.org/10.1109/I2CT51068.2021.9418154.

[22] H. Chen, C. Tan, Z. Lin, and T. Wu, "Detection of melamine adulteration in milk by near-infrared spectroscopy and one-class partial least squares," *Spectrochimica Acta Part A: Molecular and Biomolecular Spectroscopy*, vol. 173, pp. 832–836, Feb. 2017, https://doi.org/10.1016/j.saa.2016.10.051.

[23] J. K. F. Torres *et al.*, "Technological aspects of lactose-hydrolyzed milk powder," *Food Research International*, vol. 101, pp. 45–53, Nov. 2017, https://doi.org/10.1016/j.foodres.2017.08.043.

[24] S. N. Jha, P. Jaiswal, M. K. Grewal, M. Gupta, and R. Bhardwaj, "Detection of Adulterants and Contaminants in Liquid Foods—A Review," *Critical Reviews in Food Science and Nutrition*, vol. 56, no. 10, pp. 1662–1684, Jul. 2016, https://doi.org/10.1080/10408398.2013.798257.

[25] B. T. Pham, D. Tien Bui, I. Prakash, and M. B. Dholakia, "Hybrid integration of Multilayer Perceptron Neural Networks and machine learning ensembles for landslide susceptibility assessment at Himalayan area (India) using GIS," *CATENA*, vol. 149, pp. 52–63, Feb. 2017, https://doi.org/10.1016/j.catena.2016.09.007.

[26] J. S. Farah *et al.*, "Differential scanning calorimetry coupled with machine learning technique: An effective approach to determine the milk authenticity," *Food Control*, vol. 121, Mar. 2021, Art. no. 107585, https://doi.org/10.1016/j.foodcont.2020.107585.

[27] S. Kimbahune, S. M. Ghouse, M. B. S, S. Shinde, and A. K. Jha, "Hyperspectral sensing based analysis for determining milk adulteration," in *SPIE Commerical Sensing and Imaging*, Baltimore, MD, USA, Apr. 2016, vol. 9860, pp. 44–51, https://doi.org/10.1117/12.2223439.

[28] S. Tripathy, M. S. Reddy, S. R. K. Vanjari, S. Jana, and S. G. Singh, "A Step Towards Miniaturized Milk Adulteration Detection System: Smartphone-Based Accurate pH Sensing Using Electrospun Halochromic Nanofibers," *Food Analytical Methods*, vol. 12, no. 2, pp. 612–624, Feb. 2019, https://doi.org/10.1007/s12161-018-1391-y.

[29] H. A. Neto, W. L. F. Tavares, D. C. S. Z. Ribeiro, R. C. O. Alves, L. M. Fonseca, and S. V. A. Campos, "On the utilization of deep and ensemble learning to detect milk adulteration," *BioData Mining*, vol. 12, no. 1, Jul. 2019, Art. no. 13, https://doi.org/10.1186/s13040-019-0200-5.

[30] G. Durante, W. Becari, F. A. S. Lima, and H. E. M. Peres, "Electrical Impedance Sensor for Real-Time Detection of Bovine Milk Adulteration," *IEEE Sensors Journal*, vol. 16, no. 4, pp. 861–865, Oct. 2016, https://doi.org/10.1109/JSEN.2015.2494624.

[31] M. Grossi, C. Parolin, B. Vitali, and B. Ricco, "Electrical Impedance Spectroscopy (EIS) characterization of saline solutions with a low-cost portable measurement system," *Engineering Science and Technology, an International Journal*, vol. 22, no. 1, pp. 102–108, Feb. 2019, https://doi.org/10.1016/j.jestch.2018.08.012.

[32] C. Soares, J. A. Tenreiro Machado, A. M. Lopes, E. Vieira, and C. Delerue-Matos, "Electrochemical impedance spectroscopy characterization of beverages," *Food Chemistry*, vol. 302, Jan. 2020, Art. no. 125345, https://doi.org/10.1016/j.foodchem.2019.125345.

[33] C. Qin, Y. Zhang, F. Bao, C. Zhang, P. Liu, and P. Liu, "XGBoost Optimized by Adaptive Particle Swarm Optimization for Credit Scoring," *Mathematical Problems in Engineering*, vol. 2021, Mar. 2021, Art. no. e6655510, https://doi.org/10.1155/2021/6655510.

[34] A. Kehili, K. Dabbabi, and A. Cherif, "Early Detection of Parkinson's and Alzheimer's Diseases using the VOT_Mean Feature," *Engineering, Technology & Applied Science Research*, vol. 11, no. 2, pp. 6912–6918, Apr. 2021, https://doi.org/10.48084/etasr.4038.

[35] G.-B. Huang, Q.-Y. Zhu, and C.-K. Siew, "Extreme learning machine: Theory and applications," *Neurocomputing*, vol. 70, no. 1, pp. 489–501, Dec. 2006, https://doi.org/10.1016/j.neucom.2005.12.126.

[36] D. K. Singh and M. Shrivastava, "Evolutionary Algorithm-based Feature Selection for an Intrusion Detection System," *Engineering, Technology & Applied Science Research*, vol. 11, no. 3, pp. 7130–7134, Jun. 2021, https://doi.org/10.48084/etasr.4149.

[37] S. R. Gopi and M. Karthikeyan, "Effectiveness of Crop Recommendation and Yield Prediction using Hybrid Moth Flame Optimization with Machine Learning," *Engineering, Technology & Applied Science Research*, vol. 13, no. 4, pp. 11360–11365, Aug. 2023, https://doi.org/10.48084/etasr.6092.

[38] H. Badem, A. Basturk, A. Caliskan, and M. E. Yuksel, "A new efficient training strategy for deep neural networks by hybridization of artificial bee colony and limited–memory BFGS optimization algorithms," *Neurocomputing*, vol. 266, pp. 506–526, Nov. 2017, https://doi.org/10.1016/j.neucom.2017.05.061.

[39] N. K. Al-Shammari *et al.*, "Cardiac Stroke Prediction Framework using Hybrid Optimization Algorithm under DNN," *Engineering, Technology & Applied Science Research*, vol. 11, no. 4, pp. 7436–7441, Aug. 2021, https://doi.org/10.48084/etasr.4277.